

Single-cell analysis of angiotensin-converting enzyme II expression in human kidneys and bladders reveals a potential route of 2019 novel coronavirus infection

Wei Lin¹, Jue Fan², Long-Fei Hu², Yan Zhang², Joshua D. Ooi³, Ting Meng⁴, Peng Jin⁵, Xiang Ding⁵, Long-Kai Peng⁶, Lei Song⁶, Rong Tang⁶, Zhou Xiao⁴, Xiang Ao⁴, Xiang-Cheng Xiao⁴, Qiao-Ling Zhou⁴, Ping Xiao⁴, Yong Zhong⁴

¹Department of Pathology, Xiangya Hospital, Central South University, Changsha, Hunan 410008, China;

²Department of Bioinformatics and Data Science, Singleron Biotechnologies, Nanjing, Jiangsu 210032, China;

³Centre for Inflammatory Diseases, Monash University Department of Medicine, Monash Medical Centre, Clayton, VIC 3168, Australia;

⁴Department of Nephrology, Xiangya Hospital, Central South University, Changsha, Hunan 410008, China;

⁵Department of Organ Transplantation, Xiangya Hospital, Central South University, Changsha, Hunan 410008, China;

⁶Department of Kidney Transplantation, The Second Xiangya Hospital of Central South University, Changsha, Hunan 410011, China.

Abstract

Background: Since 2019, a novel coronavirus named 2019 novel coronavirus (2019-nCoV) has emerged worldwide. Apart from fever and respiratory complications, acute kidney injury has been observed in a few patients with coronavirus disease 2019. Furthermore, according to recent findings, the virus has been detected in urine. Angiotensin-converting enzyme II (ACE2) has been proposed to serve as the receptor for the entry of 2019-nCoV, which is the same as that for the severe acute respiratory syndrome. This study aimed to investigate the possible cause of kidney damage and the potential route of 2019-nCoV infection in the urinary system.

Methods: We used both published kidney and bladder cell atlas data and new independent kidney single-cell RNA sequencing data generated in-house to evaluate *ACE2* gene expression in all cell types in healthy kidneys and bladders. The Pearson correlation coefficients between *ACE2* and all other genes were first generated. Then, genes with *r* values larger than 0.1 and *P* values smaller than 0.01 were deemed significant co-expression genes with *ACE2*.

Results: Our results showed the enriched expression of *ACE2* in all subtypes of proximal tubule (PT) cells of the kidney. *ACE2* expression was found in 5.12%, 5.80%, and 14.38% of the proximal convoluted tubule cells, PT cells, and proximal straight tubule cells, respectively, in three published kidney cell atlas datasets. In addition, *ACE2* expression was also confirmed in 12.05%, 6.80%, and 10.20% of cells of the proximal convoluted tubule, PT, and proximal straight tubule, respectively, in our own two healthy kidney samples. For the analysis of public data from three bladder samples, *ACE2* expression was low but detectable in bladder epithelial cells. Only 0.25% and 1.28% of intermediate cells and umbrella cells, respectively, had *ACE2* expression.

Conclusion: This study has provided bioinformatics evidence of the potential route of 2019-nCoV infection in the urinary system.

Keywords: 2019-nCoV; Acute kidney injury; Angiotensin-converting enzyme 2; Bladder; COVID-19; Kidney; RNA sequence analysis; Single-cell analysis

Introduction

In 2019, mysterious pneumonia cases emerged and rapidly spread across the globe. Deep sequencing analysis and etiological investigations then confirmed that the pathogen was a type of newly identified coronavirus that had been labeled 2019 novel coronavirus (2019-nCoV). The rapid spread of 2019-nCoV has caused the outbreak of pneumonia worldwide, making it a severe threat

to international public health security within a short period.^[1-3]

Based on bioinformatics analyses, it has been shown that the 2019-nCoV genome is 88% identical to two bat-derived severe acute respiratory syndrome (SARS)-like coronaviruses (bat-SL-CoVZC45 and bat-SL-CoVZXC21), 79% identical to SARS-CoV, and 50% identical to Middle East respiratory syndrome coronavirus (MERS-CoV).^[4] Protein structural analyses revealed that

Access this article online

Quick Response Code:



Website:
www.cmj.org

DOI:
10.1097/CM9.0000000000001439

Correspondence to: Prof Yong Zhong, Department of Nephrology, Xiangya Hospital, Central South University, Changsha, Hunan 410008, China
E-Mail: zhongyong121@163.com

Copyright © 2021 The Chinese Medical Association, produced by Wolters Kluwer, Inc. under the CC-BY-NC-ND license. This is an open access article distributed under the terms of the Creative Commons Attribution-Non Commercial-No Derivatives License 4.0 (CCBY-NC-ND), where it is permissible to download and share the work provided it is properly cited. The work cannot be changed in any way or used commercially without permission from the journal.

Chinese Medical Journal 2021;134(8)

Received: 16-11-2020 Edited by: Peng Lyu

2019-nCoV had a receptor-binding domain similar to that of SARS-CoV, directly binding to angiotensin-converting enzyme II (ACE2), strongly suggesting that 2019-nCoV uses ACE2 as its receptor.^[5-8]

The most common symptoms of 2019-nCoV infection are fever and cough in most patients, with symptoms of chest discomfort, progressive dyspnea, or acute respiratory distress syndrome (ARDS) in severe patients. Acute kidney injury (AKI) has been reported in a small number of patients with confirmed 2019-nCoV infection. The laboratory findings of 99 patients infected with 2019-nCoV showed that three patients (3%) had different degrees of increased serum creatinine.^[9] In another clinical observation study, four (10%) of 41 patients, including two of 13 (15%) intensive care unit (ICU) patients and two of 28 (7%) non-ICU patients, showed elevated serum creatinine.^[10] A total of 3.7% of patients died of renal failure as shown in an analysis of 88 coronavirus disease 2019 (COVID-19)-related deaths.^[11] Additionally, the latest research confirmed that 27.06% (23/85) of patients exhibited acute renal failure, and severe acute tubular necrosis was observed by hematoxylin-eosin staining in six patients post-mortem. The 2019-nCoV antigen was detected in kidney tubules by immunohistochemistry (IHC) as well.^[12] Moreover, 2019-nCoV was detected in urine samples by quantitative real-time polymerase chain reaction of a patient with a 2019-nCoV infection.^[13,14] However, why and how 2019-nCoV induces AKI in urine remains largely unknown. Also, whether 2019-nCoV can be transmitted through the urinary tract remains a largely unanswered question. As ACE2 plays an important role in 2019-nCoV infection, we aimed to identify the ACE2-expressing cell composition and proportion in normal human kidneys and bladders by single-cell transcriptomes to explore the possible infection routes of 2019-nCoV and the roles of ACE2 in urinary tract system infection.

Single-cell RNA sequencing (scRNA-Seq) has been extensively applied in 2019-nCoV research due to its capability to profile gene expression for all cell types in multiple tissues unbiasedly at a high resolution. The expression of ACE2 has been investigated in the well-known alveolar type 2 cells in the lung as well as in liver cholangiocytes, esophageal epithelial cells, and absorptive enterocytes of the ileum and colon by scRNA-Seq.^[15-17] These results demonstrated the potential utility of scRNA-Seq to unmask the potential target cell types of 2019-nCoV. Since urinary system infection and its potential aftermath could be essential to patient care during and after infection, we used two scRNA-Seq transcriptome datasets in healthy kidneys and one dataset in healthy bladders to investigate the expression patterns of cell types in the urinary system.

Methods

Public dataset acquisition and processing

Gene expression matrices of scRNA-Seq data from normal kidneys of three healthy donors were downloaded from the Gene Expression Omnibus (GSE131685). We reproduced the downstream analysis using the code provided by the author in the original paper.

We obtained the scRNA-Seq data of healthy bladder tissues of three bladder cancer patients from the Gene Expression Omnibus (GSE108097). To be consistent with the kidney datasets, we applied Harmony (The Harmony method is an algorithm for performing integration of single cell genomics datasets for batch correction and meta analysis, which is fast, sensitive, and accurate. It can also remove the influence of dataset-of-origin from the embedding.)^[18] to integrate samples and performed downstream analysis using Seurat (version 3.1, Satija Lab, <https://satijalab.org/seurat/>). All gene expression was normalized and scaled using NormalizeData and ScaleData (NormalizeData is a function of Seurat which can normalize the count data present in a given assay. ScaleData is a function of Seurat which can scale and center genes in the dataset, standardize the range of expression values across all the genes.). Top 2000 variable genes were selected by FindVariableFeatures for principal components analysis. Clustering analysis using FindClusters was performed by first reducing the gene expression matrix to the first 20 principal components and then using a resolution of 0.3 for graph-based clustering.

Kidney sample processing

Kidney samples were obtained at a single site by wedge and needle biopsy of living donor kidneys after removal from the donor and before implantation in the recipient. Kidney samples were obtained at a single site by wedge and needle biopsy of living donor kidneys after removal from the donor and before implantation in the recipient. All procedures involving human participants were performed in accordance with the ethical standards of the Ethics Committee of Xiangya Hospital of Central South University (IRB approval number 201711836) and with the 1964 *Declaration of Helsinki* and its later amendments or comparable ethical standards. Kidney biopsy samples were cleaned with sterile phosphate buffer saline (PBS) after the acquisition.

Tissue dissociation

Fresh kidney tissue was immediately transferred into GEXSCOPE[®] Tissue Preservation Solution (Singleron Biotechnologies, Nanjing, Jiangsu Province, China) at 2°C to 8°C. The samples were digested in 2 mL of GEXSCOPE[®] tissue dissociation solution (Singleron Biotechnologies) at 37°C for 15 min in a 15-mL centrifuge tube with continuous agitation after being washed with Hanks balanced salt solution three times and cut into approximately 1 to 2 mm pieces. Subsequently, cell debris and other impurities were filtered by a 40-micron sterile strainer (Corning, NY, USA). The cells were centrifuged at 300 × g and 4°C for 5 min. Cell pellets were resuspended in 1 mL of PBS (HyClone, Marlborough, MA, USA). To remove red blood cells, 2 mL GEXSCOPE[®] Red Blood Cell Lysis Buffer (Singleron Biotechnologies) was added to the cell suspension and incubated at 25°C for 10 min. The mixture was then centrifuged at 500 × g for 5 min, and the cell pellet was resuspended in PBS. Cells were counted with a TC20 automated cell counter (Bio-Rad, Hercules, CA, USA).

Library preparation and data analysis of scRNA-Seq

The single-cell suspension was subjected to single-cell library preparation and sequencing, as previously described.^[19] To be consistent with the public data used above, we applied a similar downstream analysis workflow.^[18] We modified the number of principal components to 20 and used a resolution of 0.6 to obtain comparable cell type clustering results with

the public kidney data. Cell types were annotated based on canonical markers in the literature.^[18,20]

Co-expression, pathway enrichment, and protein interaction analyses

For each dataset, we used all cells of selected cell types and calculated co-expressed genes with ACE2 (three

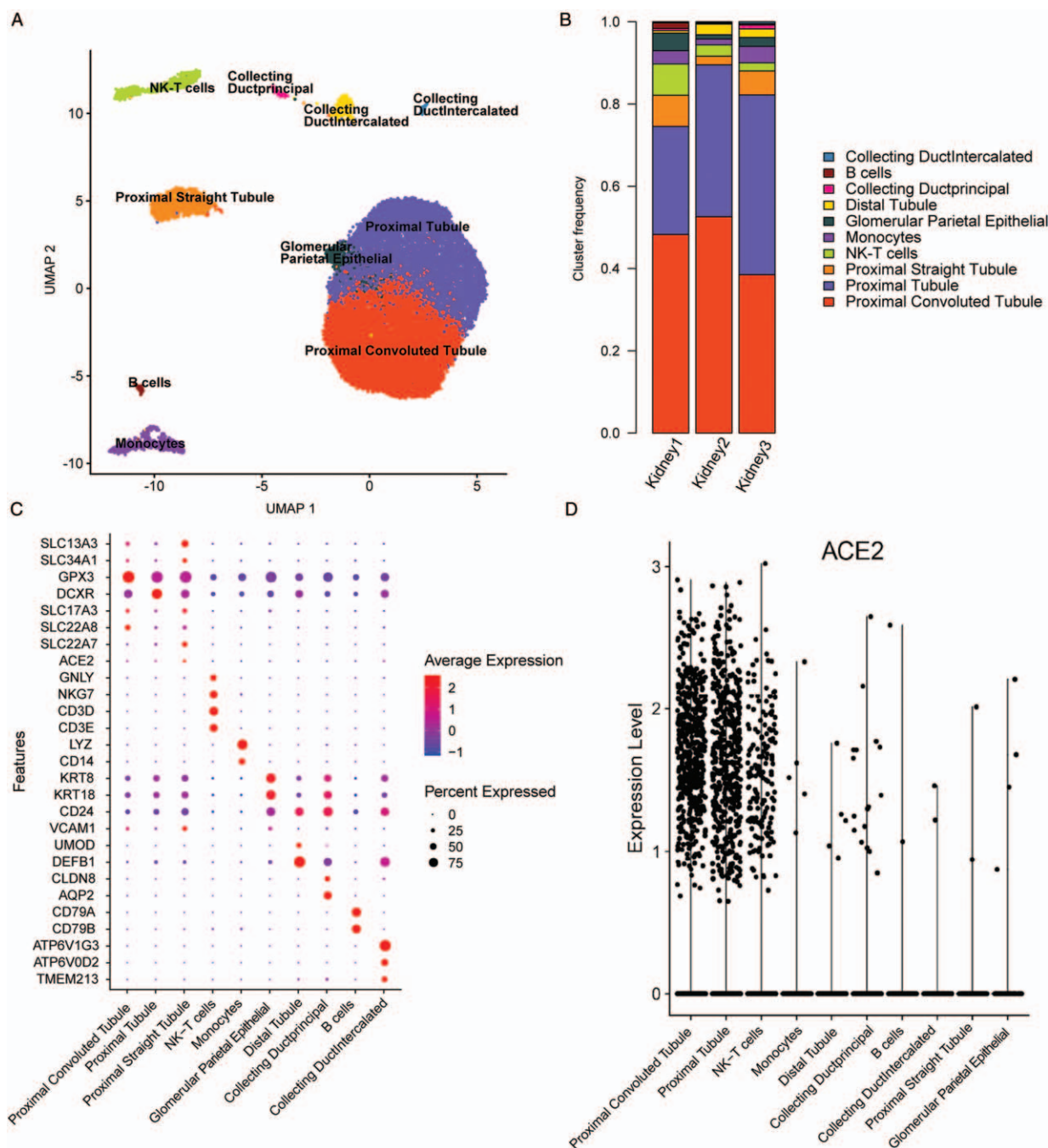


Figure 1: Single-cell analysis of public kidney data from three donors. (A) UMAP plot revealing the cell type annotations of three samples. (B) The cellular composition of three healthy kidney samples. Proximal convoluted tubule cells accounted for 48.3%, 52.6%, and 38.5%; PT cells accounted for 26.3%, 36.9%, and 43.7%; and proximal straight tubule cells accounted for 7.6%, 2.1%, and 5.8%. (C) Dot plot exhibiting canonical markers used for cell-type classification. The abscissa represents each cell type, the ordinate represents marker genes, the color of the dot in the figure represents the level of expression, and the size of the dot represents the proportion of gene expression in the cell. (D) The gene expression patterns of ACE2 of all detected cell types in the kidney. The cell type is represented horizontally, and the ACE2 expression value is represented vertically. Each point represents one cell. The cells that mainly expressed ACE2 in the kidney samples are PT cells. ACE2: Angiotensin-converting enzyme II; PT: Proximal tubule; UMAP: Uniform manifold approximation and projection.

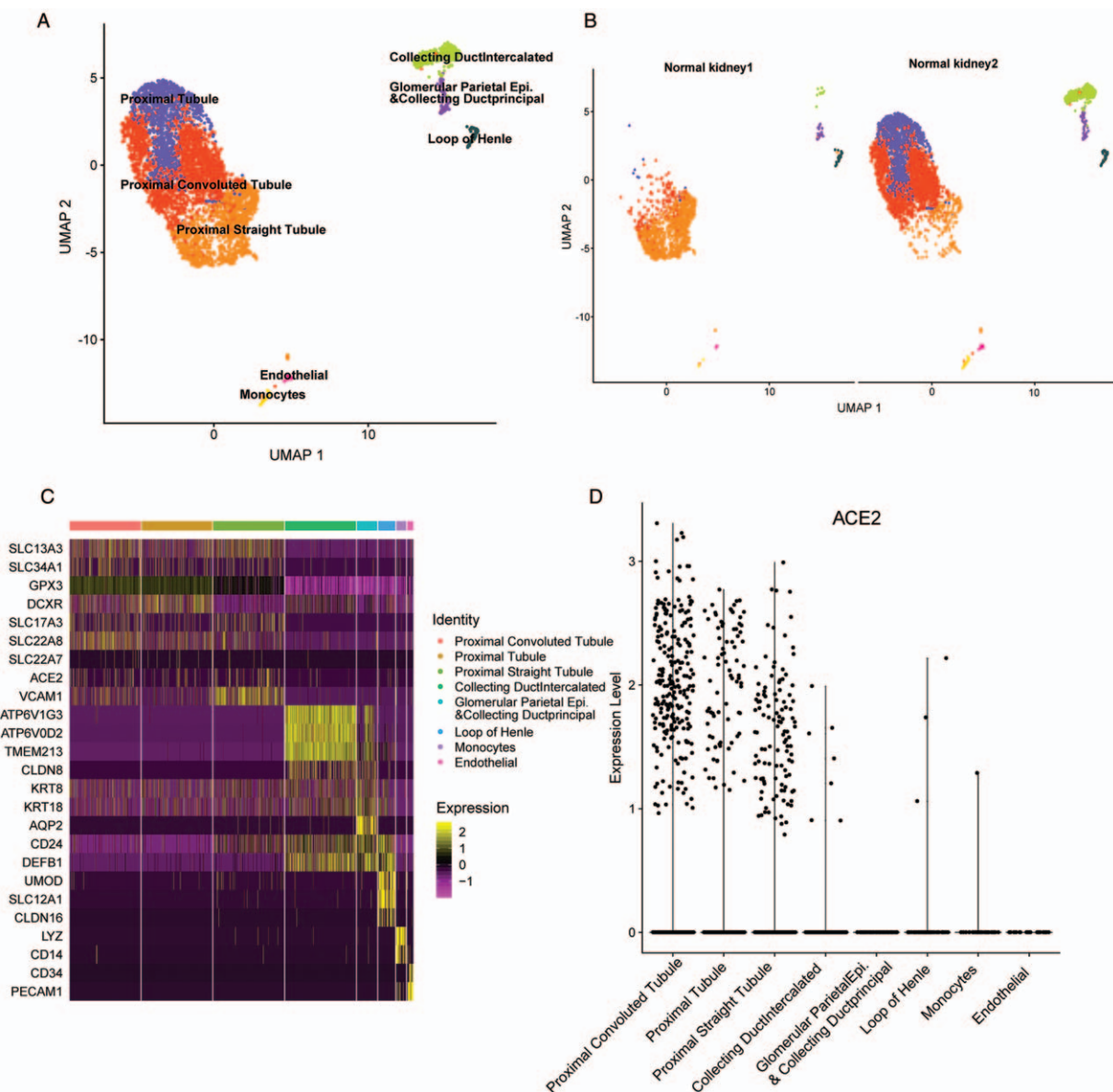


Figure 2: Single-cell analysis of the two kidney biopsy samples. (A) Cell type annotations visualized by UMAP. The different cell types are color-coded, and cell names were added. (B) Sample-specific UMAP visualization of two samples. Cell types are distinguished by different colors. (C) Heatmap of canonical markers applied for cell type assignment. The cell type is represented horizontally, the gene list is represented vertically, and the expression level is represented by color in the figure. (D) Violin plot displaying the expression signals of kidney cell types. The cell type is represented horizontally, and the ACE2 expression value is represented vertically. Each scatter point represented one cell. The cells that mainly expressed ACE2 in the kidney samples are PT cells. ACE2: Angiotensin-converting enzyme II; PT: Proximal tubule; UMAP: Uniform manifold approximation and projection.

proximal tubule [PT] cells for kidney and umbrella cells for bladder). The Pearson correlation coefficients between *ACE2* and all other genes were first generated. Then, genes with *r* values larger than 0.1 and *P* values smaller than 0.01 were deemed significant co-expression genes with *ACE2*. We removed mitochondrial genes for the following pathway enrichment and protein-protein interaction (PPI) analyses. For kidney datasets, we used the co-expressed genes in at least two out of three cell types of the PT, proximal straight tubule, and proximal convoluted tubule cells in a Venn diagram. A total of 126 and 65 genes remained for the public and private kidney datasets, respectively. For the bladder dataset, the final set contained 372 genes. Gene Ontology (GO) and Kyoto

Encyclopedia of Genes and Genomes (KEGG) pathway enrichment analyses were applied using the R package ClusterProfiler (version 3.8.1, Bioconductor, <https://bioconductor.org/packages/release/bioc/html/clusterProfiler.html>). Pathways with *P*_{adj} value less than 0.05 were considered as significantly enriched. For PPI analysis, two final sets of genes from two kidney datasets were combined to form a 170-gene list. PPI analysis was predicted based on known interactions of genes with relevant GO terms in the R package STRINGdb (version 1.20.0, <https://string-db.org/>). Based on the differentially upregulated gene protein interaction network data, the PPI network was exported using Cytoscape software (version 3.4, <https://cytoscape.org/>).

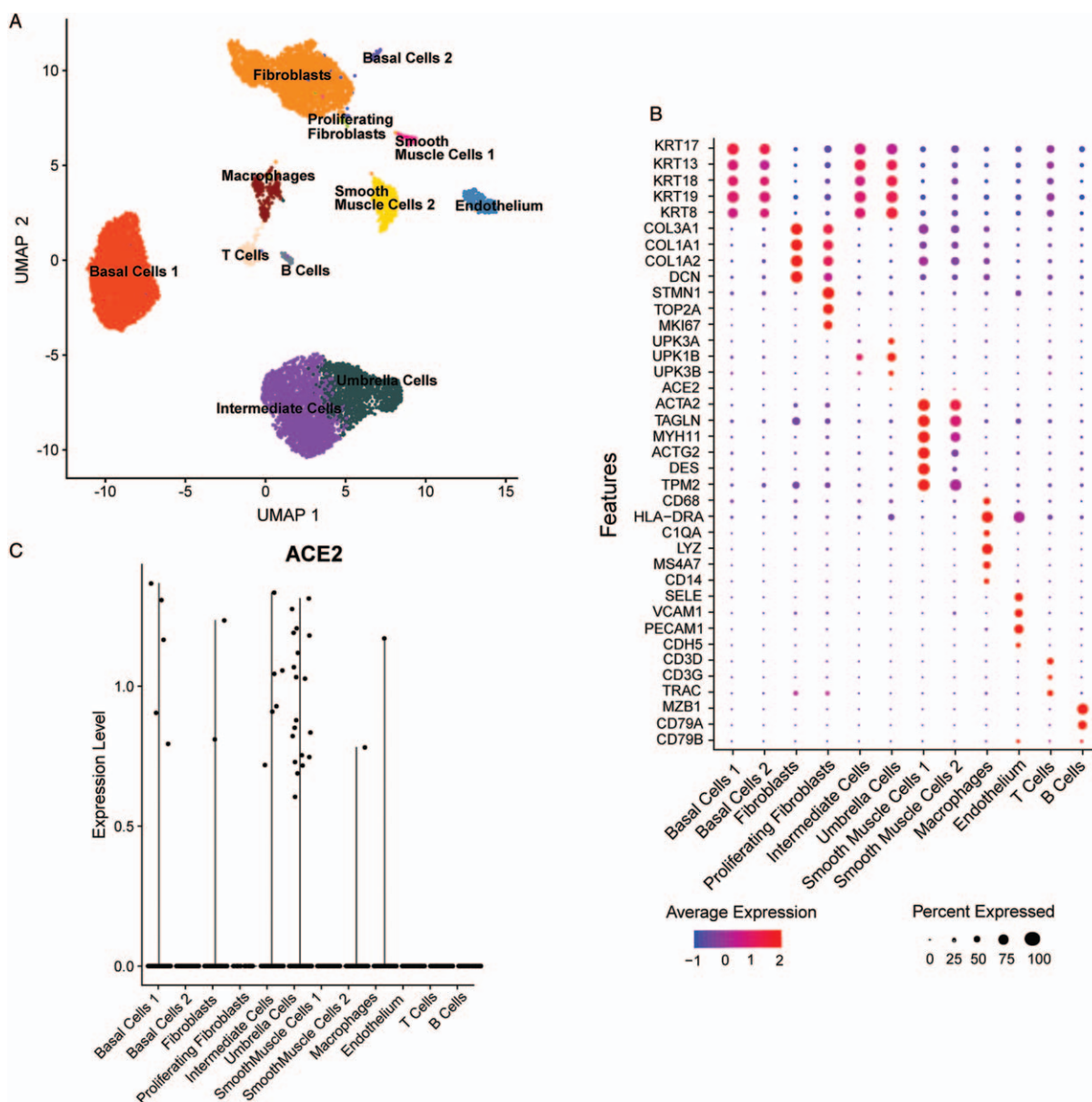


Figure 3: Public bladder single-cell dataset. (A) Two-dimensional visualization of the bladder cell atlas by UMAP. The different cell types are color-coded, and the cell names were added. (B) Expression pattern of canonical markers used for identifying bladder cell types. The X-axis represents each cell type, the Y-axis represents marker genes, the color of the dot in the figure represents the level of expression, and the size of the dot represents the proportion of gene expression in the cell. (C) ACE2 expression across 12 cell subgroups in the bladder dataset. The cell type is on the horizontal axis, and the ACE2 expression value is represented vertically. Each scatter point represented one cell. ACE2 is expressed in umbrella cells in bladder samples. ACE2: Angiotensin-converting enzyme II; UMAP: Uniform manifold approximation and projection.

Statistical analysis

Marker genes for each cluster were identified with the Wilcox likelihood-ratio test with default parameters via the FindAllMarkers function in Seurat v.3.1.2. Marker genes that are expressed in >10% of the cells in a cluster and average log (fold change) of >0.25 were selected. Pearson correlation was used to analyze significantly co-expressed genes with ACE2, and a P value smaller than 0.01 was used to identify significantly co-expressed genes with ACE2. For the scRNA-Seq data, statistical analysis and figures were completed by R (version 3.5.1, <https://www.r-project.org/>).

Results

Expression patterns of ACE2 in kidney

By analyzing the public single-cell transcriptome dataset of normal human kidney cells from three donors, we found that ACE2 expression was distributed across multiple cell types. Notably, ACE2 was mostly enriched in PT cells, including both convoluted tubules and straight tubules [Figure 1A–1D]. The other nephron subtypes, such as collecting duct and distal tubule as well as immune cells, all showed extremely low gene expression.

To validate this result, we further analyzed normal kidney samples from two healthy donors. The 4736 cells were classified into nine cell types, which highly overlapped with public data, including seven nephron-specific subtypes based on canonical marker genes [Figure 2A]. The PT (*CUBN*, *SLC13A3*, and *SLC22A8*) was classified into proximal convoluted tubule and proximal straight tubule based on different marker expression levels.^[18,20] Collecting duct principal cells (*AQP2*), collecting duct intercalated cells (*ATP6V0D2*), and glomerular parietal epithelial cells (*KRT8* and *KRT18*) were also annotated, and these results are in line with the previous result. Furthermore, we identified a cluster of loops of Henle cells (*UMOD*, *SLC12A1*, and *CLDN16*), which was absent in the public dataset. Additionally, the stroma and immune cells, composed of a small number of endothelial cells (*CD34* and *PECAM1*) and monocytes (*CD14*, *FCN1*, and *VCAN*), were found [Figure 2B]. The representative marker genes for all subpopulations are plotted in Figure 2C.

As observed in the public dataset, we observed upregulated *ACE2* expression in all PT cells compared with other cell types [Figure 2D]. Quantitatively, *ACE2* expression was also confirmed in 12.05%, 6.79%, and 10.20% of cells of the proximal convoluted tubule, PT, and proximal straight tubule, respectively, in our own two healthy normal kidney samples. Previous IHC analysis^[21] indicated a complex spatial distribution of *ACE2* protein expression concentrated in the brush border of the PTs.

Expression pattern of *ACE2* in the bladder

Based on the public bladder dataset of 12 cell types [Figure 3A and 3B], we found low expression of *ACE2* in all epithelial cell types. The concentration of *ACE2* seemed to have a decreasing trend from the outer layer of the bladder epithelium (umbrella cells) to the inner layer (basal cells) with the intermediate cells in-between. Other cell types, such as endothelial and immune cells, are mostly negative for *ACE2* [Figure 3C]. The percentage of umbrella cells in the bladder expressing *ACE2* (1.3%) was lower than that in the renal epithelium. A previous analysis of SARS patients indicated that the SARS virus (SARS-CoV) was able to survive in urine at detectable levels.^[22,23] The detection of SARS-CoV in urine implied the possibility of virus release from infected bladder epithelial cells, which is in agreement with our analysis above.

Functional analysis of co-expressed genes with *ACE2*

In both kidney datasets, we found a large number of genes co-expressed with *ACE2*, especially in proximal straight tubule cells [Figure 4A and 4D]. The co-expressed genes were enriched in multiple membrane-related cellular components (CC) [Figure 4B and 4E]. Notably, brush border and brush border membranes were significantly enriched CC terms, which aligns well with the cellular locations of *ACE2* detected by immunohistochemical analysis.^[21] The enriched KEGG terms included the normal functions of *ACE2*, such as the renin-angiotensin system, PT

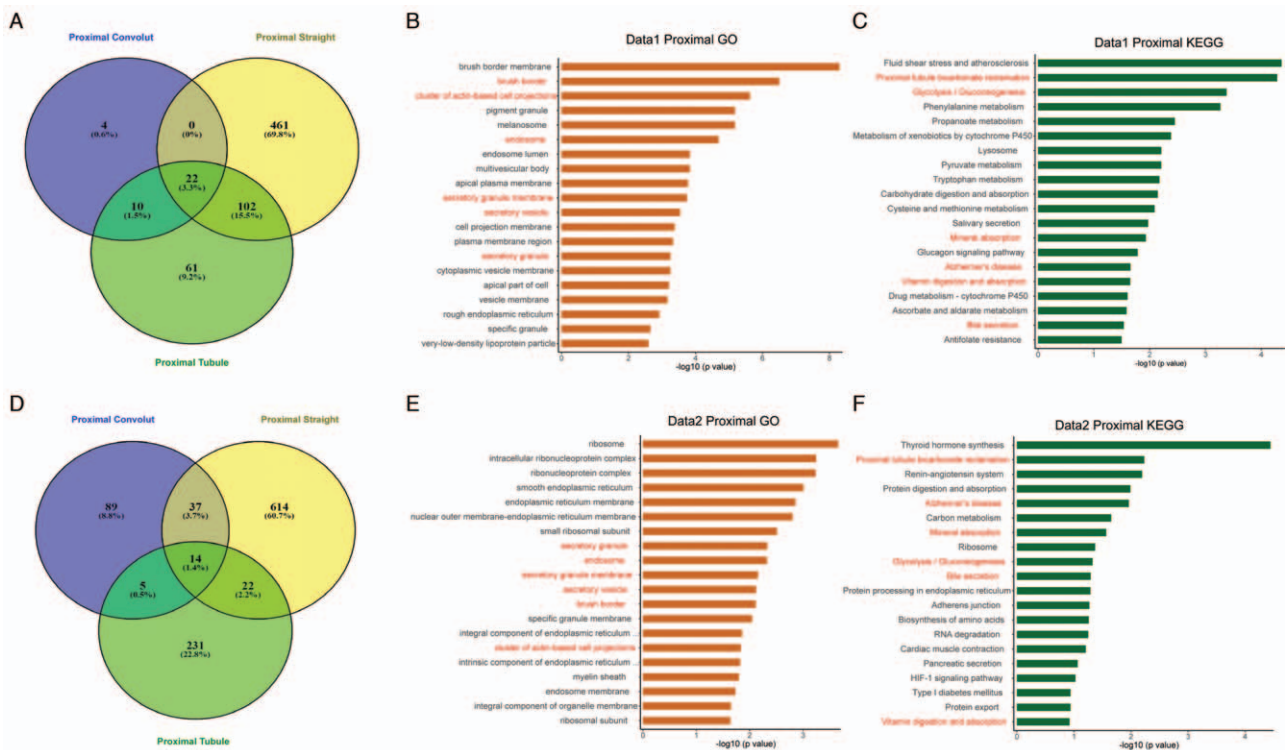


Figure 4: Functional analysis of *ACE*-related genes in the kidney. (A, D) Venn diagram of *ACE2* co-expression genes from three PT cells in the public kidney dataset (Data 1) and the private kidney dataset (Data 2). (B, E) Analysis of *ACE2* co-expression genes in each cell (expression related to >2 cell types) for GO CC term enrichment in Data 1 and Data 2. The X-axis represents the log-transformed P values. (C, F) Analysis of *ACE2* co-expression genes for KEGG term enrichment in Data 1 and Data 2. The term in red is the common path between the data sets. *ACE2*: Angiotensin-converting enzyme II; CC: Cellular components; GO: Gene Ontology; KEGG: Kyoto Encyclopedia of Genes and Genomes; PT: Proximal tubule.

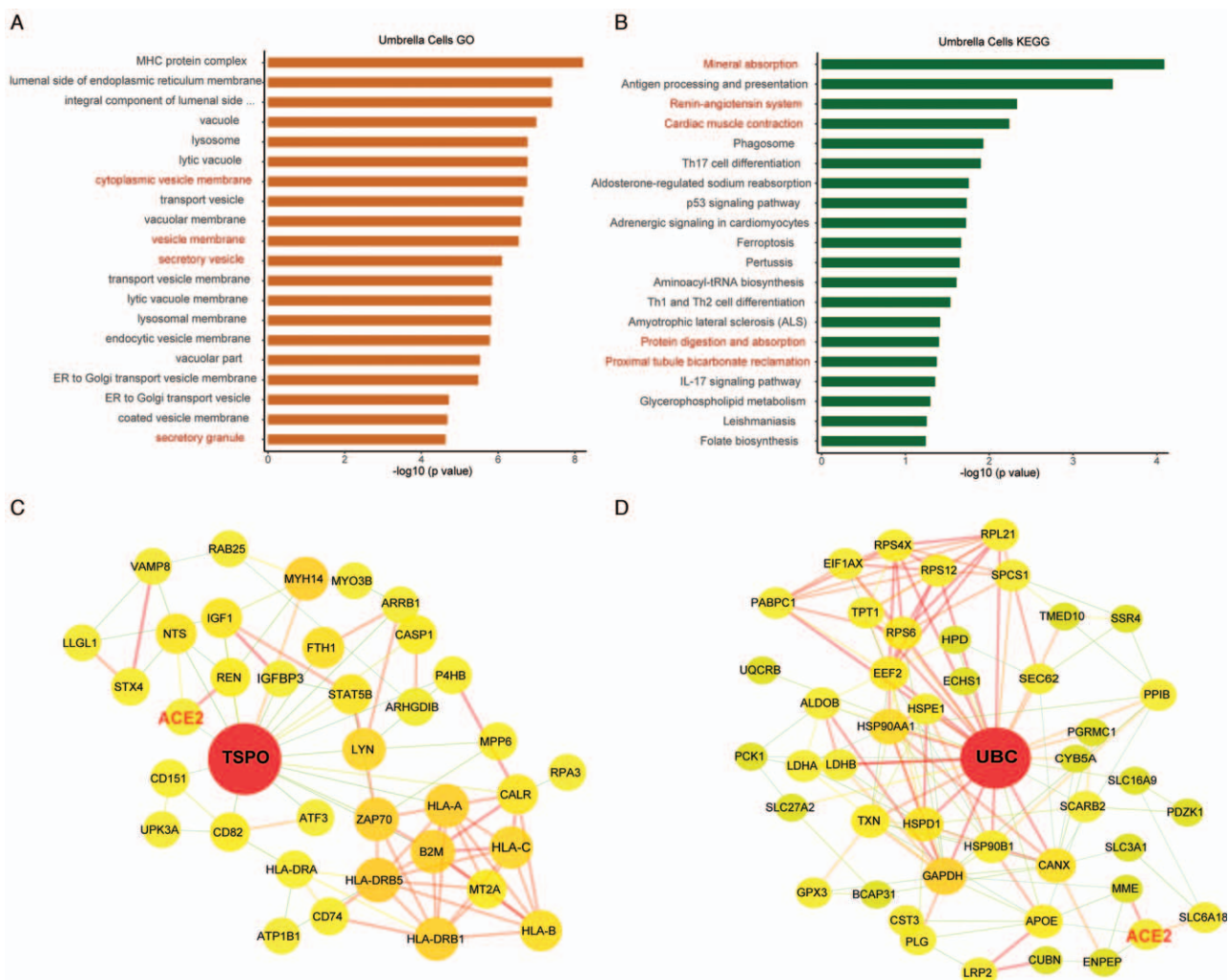


Figure 5: Functional analysis of ACE2-related genes in the bladder. (A) Analysis of ACE2 co-expression genes in umbrella cells of the bladder for GO CC term enrichment. The X-axis represents the log-transformed P values. (B) Analysis of ACE2 co-expression genes in umbrella cells of the bladder for KEGG term enrichment. (C, D) PPI networks displaying the relationships between ACE2 and its related genes in kidneys and bladders. The size of the node (gene) represents the number of interaction partners (neighbors). The line width and the color (narrow to wide corresponding to blue to red) are proportional to the interacting strength in the STRING database. ACE2: Angiotensin-converting enzyme II; CC: Cellular components; GO: Gene Ontology; KEGG: Kyoto Encyclopedia of Genes and Genomes; PPI: Protein-protein interaction.

bicarbonate reclamation, mineral absorption, and multiple metabolism-related pathways [Figure 4C and 4F]. The results confirmed that ACE2 and its related genes are essential to maintain the functionality of the kidney.^[24] For the bladder dataset, the CC and KEGG enrichment results were generally consistent with those of kidneys, where membrane proteins and renal functions such as absorption and metabolism were involved [Figure 5A and 5B]. We performed PPI analysis for ACE2 and its co-expressed genes in both the kidney and bladder, as shown in Figure 5C and 5D. Whether these interacting proteins are involved in the pathogenic changes of PT and umbrella cell infections is unclear and needs to be further investigated.

Discussion

AKI in 2019-nCoV and SARS-CoV infection

COVID-19 is a new infectious disease with a formidable speed of transmission. While most of these patients exhibit

respiratory symptoms, a wide range of non-respiratory symptoms have also been reported, demonstrating that other organs are affected during the disease. In the analysis of the clinical features of patients infected with 2019-nCoV, renal function damage has been confirmed,^[9,10] and continuous kidney substitution treatment was needed in approximately 9% of all 99 infected patients.^[9] Gabarre *et al*^[25] systematically reviewed AKI in critically ill patients with COVID-19. Besides, kidney injury and renal dysfunction have been observed in other coronaviruses associated with respiratory infections, especially two beta-coronaviruses (SARS-CoV and MERS-CoV),^[26] which are genetically similar to 2019-nCoV.^[4,8] A previous study reported that 36 (6.7%) of 536 patients with SARS developed AKI, and 33 of all 36 patients (91.7%) with renal dysfunction died.^[27] Importantly, SARS-CoV fragments have been detected by polymerase chain reaction in urine specimens of some patients.^[28] Furthermore, persistent SARS-CoV infection and replication have been observed in the kidney particularly in tubular epithelial cells *in vitro*,^[29] indicating that kidney damage in patients

with SARS could be due to direct viral infection in target cells except for other triggers, such as the host immune response, severe pneumonia, and ARDS. While very similar pathogenically to SARS-CoV, the detailed mechanism of renal involvement of 2019-nCoV remains unclear.

Analysis of ACE2 expression in the urinary system

The etiology of AKI in SARS seems to be multifactorial and still uncertain, which was thought to have a certain correlation with the high expression of ACE2 in the kidney.^[29,30] scRNA-seq, a new approach that is increasingly used in the field of biology and medicine, can analyze cell types and expression genes at the cellular level. Based on our single-cell analysis in both normal kidneys (both the public and our data) and bladders, we found detectable levels of ACE2 in both the kidney and bladder. Similar to our data, Deng and coworkers^[31] analyzed public kidney data and suggested that the kidney is at high risk of coronavirus infection. Moreover, in our data, we found that PT cells have higher expression percentages than bladder epithelial cells, which may indicate that the kidney is more susceptible to 2019-nCoV infection than the bladder. Compared to the expression levels of ACE2 in the digestion system,^[15] the lower expression of ACE2 in the urinary system could suggest fewer patients with renal-related symptoms, which positively correlates with the observations for SARS patients. The co-expression and pathway analysis revealed critical functions of ACE2 in the urinary system, which may explain the dysfunction of the kidney caused by ACE2-binding viruses. Moreover, ACE2 expression in exterior cells (PT cells in renal tubules and umbrella cells in bladder epithelium) may also be one of the causes of the presence of viruses in the urine.

Significance of the study

AKI, which has been proven to be a predictor of high mortality in SARS patients,^[27] may also lead to difficulty of treatment, worsening conditions, and even be a negative prognostic indicator for the survival of 2019-nCoV infected patients. The present study provided direct evidence for the possible infection of renal epithelial cells with 2019-nCoV, which calls for more attention to COVID-19 patients with AKI, especially during an extensive outbreak and the global epidemic continues to deteriorate. In addition, the distribution of ACE2 in the urinary system and its detection^[32] in urine samples hinted at the necessity of virus testing in urine samples of COVID-19 patients, which could reduce the risk of transmission to some extent.

Our results must also be viewed in terms of their limitations. First, we analyzed ACE2 expression only in healthy individual samples, and the lack of samples from patients with COVID-19 is the major limitation. Furthermore, we did not include a validation cohort to confirm our findings. More direct evidence from *in vitro* experiments and patient samples is needed.

Funding

This work was supported by the Project of Health Commission of Hunan Province (No. C2019184) and

the National Natural Science Foundation of China (No. 81800641).

Conflicts of interest

None.

References

1. The Lancet. Emerging understandings of 2019-nCoV. *Lancet* 2020;395:311. doi: 10.1016/s0140-6736(20)30186-0.
2. Nishiura H, Jung S-M, Linton NM, Kinoshita R, Yang Y, Hayashi K, *et al.* The extent of transmission of novel coronavirus in Wuhan, China, 2020. *J Clin Med* 2020;9:330. doi: 10.3390/jcm9020330.
3. Li Q, Guan X, Wu P, Wang X, Zhou L, Tong Y, *et al.* Early transmission dynamics in Wuhan, China, of novel coronavirus-infected pneumonia. *N Engl J Med* 2020;382:1199–1207. doi: 10.1056/NEJMoa2001316.
4. Lu R, Zhao X, Li J, Niu P, Yang B, Wu H, *et al.* Genomic characterisation and epidemiology of 2019 novel coronavirus: implications for virus origins and receptor binding. *Lancet* 2020;395:565–574. doi: 10.1016/s0140-6736(20)30251-8.
5. Wan Y, Shang J, Graham R, Baric RS, Li F. Receptor recognition by novel coronavirus from Wuhan: an analysis based on decade-long structural studies of SARS. *J Virol* 2020;94:e00127–e00220. doi: 10.1128/jvi.00127-20.
6. Chen Y, Liu Q, Guo D. Emerging coronaviruses: genome structure, replication, and pathogenesis. *J Med Virol* 2020;92:418–423. doi: 10.1002/jmv.25681.
7. Xu X, Chen P, Wang J, Feng J, Zhou H. Evolution of the novel coronavirus from the ongoing Wuhan outbreak and modeling of its spike protein for risk of human transmission. *Sci China Life Sci* 2020;63:457–460. doi: 10.1007/s11427-020-1637-5.
8. Zhou P, Yang XL, Wang XG, Hu B, Zhang L, Zhang W, *et al.* A pneumonia outbreak associated with a new coronavirus of probable bat origin. *Nature* 2020;579:270–273. doi: 10.1038/s41586-020-2012-7.
9. Chen N, Zhou M, Dong X, Qu J, Gong F, Han Y, *et al.* Epidemiological and clinical characteristics of 99 cases of 2019 novel coronavirus pneumonia in Wuhan, China: a descriptive study. *Lancet* 2020;395:507–513. doi: 10.1016/s0140-6736(20)30211-7.
10. Huang C, Wang Y, Li X, Ren L, Zhao J, Hu Y, *et al.* Clinical features of patients infected with 2019 novel coronavirus in Wuhan, China. *Lancet* 2020;395:497–506. doi: 10.1016/s0140-6736(20)30183-5.
11. Zhang B, Zhou X, Qiu Y, Song Y, Feng F, Feng J, *et al.* Clinical characteristics of 82 cases of death from COVID-19. *PLoS One* 2020;15:e0235458. doi: 10.1371/journal.pone.0235458.
12. Diao B, Feng Z, Wang C, Wang H, Liu L, Wang C, *et al.* Human kidney is a target for novel severe acute respiratory syndrome coronavirus 2 (SARS-CoV-2) infection. *medRxiv* 2020. doi: 10.1101/2020.03.04.20031120.
13. Peng L, Liu J, Xu W, Luo Q, Chen D, Lei Z, *et al.* SARS-CoV-2 can be detected in urine, blood, anal swabs, and oropharyngeal swabs specimens. *J Med Virol* 2020;92:1676–1680. doi: 10.1002/jmv.25936.
14. Wang W, Xu Y, Gao R, Lu R, Han K, Wu G, *et al.* Detection of SARS-CoV-2 in different types of clinical specimens. *JAMA* 2020;323:1843–1844. doi: 10.1001/jama.2020.3786.
15. Zhang H, Kang Z, Gong H, Xu D, Wang J, Li Z, *et al.* The digestive system is a potential route of 2019-nCoV infection: a bioinformatics analysis based on single-cell transcriptomes. *bioRxiv* 2020. doi: 10.1101/2020.01.30.927806.
16. Zhao Y, Zhao Z, Wang Y, Zhou Y, Ma Y, Zuo W. Single-Cell RNA Expression Profiling of ACE2, the Receptor of SARS-CoV-2. *Am J Respir Crit Care Med* 2020;202:756–759. doi: 10.1164/rccm.202001-0179LE.
17. Chai X, Hu L, Zhang Y, Han W, Lu Z, Ke A, *et al.* Specific ACE2 expression in cholangiocytes may cause liver damage after 2019-nCoV infection. *bioRxiv* 2020. doi: 10.1101/2020.02.03.931766.
18. Korsunsky I, Millard N, Fan J, Slowikowski K, Zhang F, Wei K, *et al.* Fast, sensitive and accurate integration of single-cell data with Harmony. *Nat Methods* 2019;16:1289–1296. doi: 10.1038/s41592-019-0619-0.
19. Zhao X, Wu S, Fang N, Sun X, Fan J. Evaluation of single-cell classifiers for single-cell RNA sequencing data sets. *Brief Bioinform* 2019;21:1581–1595. doi: 10.1093/bib/bbz096.

20. Young MD, Mitchell TJ, Vieira Braga FA, Tran MGB, Stewart BJ, Ferdinand JR, *et al.* Single-cell transcriptomes from human kidneys reveal the cellular identity of renal tumors. *Science* 2018;361:594–599. doi: 10.1126/science.aat1699.
21. Hamming I, Timens W, Bulthuis MLC, Lely AT, Navis G, van Goor H. Tissue distribution of ACE2 protein, the functional receptor for SARS coronavirus. A first step in understanding SARS pathogenesis. *J Pathol* 2004;203:631–637. doi: 10.1002/path.1570.
22. Lau SKP, Che X-Y, Woo PCY, Wong BHL, Cheng VCC, Woo GKS, *et al.* SARS coronavirus detection methods. *Emerg Infect Dis* 2005;11:1108–1111. doi: 10.3201/eid1107.041045.
23. Chu CM, Leung WS, Cheng VCC, Chan KH, Lin AWN, Chan VL, *et al.* Duration of RT-PCR positivity in severe acute respiratory syndrome. *Eur Respir J* 2005;25:12–14. doi: 10.1183/09031936.04.00057804.
24. Mizuiri S, Ohashi Y. ACE and ACE2 in kidney disease. *World J Nephrol* 2015;4:74–82. doi: 10.5527/wjn.v4.i1.74.
25. Gabarre P, Dumas G, Dupont T, Darmon M, Azoulay E, Zafrani L. Acute kidney injury in critically ill patients with SARS-CoV-2. *Intensive Care Med* 2020;46:1339–1348. doi: 10.1007/s00134-020-06153-9.
26. Farcas GA, Poutanen SM, Mazzulli T, Willey BM, Butany J, Asa SL, *et al.* Fatal severe acute respiratory syndrome is associated with multiorgan involvement by coronavirus. *J Infect Dis* 2005;191:193–197. doi: 10.1086/426870.
27. Chu KH, Tsang WK, Tang CS, Lam MF, Lai FM, To KF, *et al.* Acute renal impairment in coronavirus-associated severe acute respiratory syndrome. *Kidney Int* 2005;67:698–705. doi: 10.1111/j.1523-1755.2005.67130.x.
28. Yam WC, Chan KH, Poon LLM, Guan Y, Yuen KY, Seto WH, *et al.* Evaluation of reverse transcription-PCR assays for rapid diagnosis of severe acute respiratory syndrome associated with a novel coronavirus. *J Clin Microbiol* 2003;41:4521–4524. doi: 10.1128/jcm.41.10.4521-4524.2003.
29. Pacciarini F, Ghezzi S, Canducci F, Sims A, Sampaolo M, Ferioli E, *et al.* Persistent replication of severe acute respiratory syndrome coronavirus in human tubular kidney cells selects for adaptive mutations in the membrane protein. *J Virol* 2008;82:5137–5144. doi: 10.1128/jvi.00096-08.
30. Lau YL, Peiris JSM. Pathogenesis of severe acute respiratory syndrome. *Curr Opin Immunol* 2005;17:404–410. doi: 10.1016/j.coi.2005.05.009.
31. Deng YY, Zheng Y, Cai GY, Chen XM, Hong Q. Single-cell RNA sequencing data suggest a role for angiotensin-converting enzyme 2 in kidney impairment in patients infected with 2019-novel coronavirus. *Chin Med J* 2020;133:1129–1131. doi: 10.1097/cm9.0000000000000783.
32. Sun J, Zhu A, Li H, Zheng K, Zhuang Z, Chen Z, *et al.* Isolation of infectious SARS-CoV-2 from urine of a SARS-CoV-2 patient. *Emerg Microbes Infect* 2020;9:991–993. doi: 10.1080/22221751.2020.1760144.

How to cite this article: Lin W, Fan J, Hu LF, Zhang Y, Ooi JD, Meng T, Jin P, Ding X, Peng LK, Song L, Tang R, Xiao Z, Ao X, Xiao XC, Zhou QL, Xiao P, Zhong Y. Single-cell analysis of angiotensin-converting enzyme II expression in human kidneys and bladders reveals a potential route of 2019 novel coronavirus infection. *Chin Med J* 2021;134:935–943. doi: 10.1097/CM9.0000000000001439